

Band gap engineering and spatial confinement of optical phonon in ZnO quantum dots

Kuo-Feng Lin, Hsin-Ming Cheng, Hsu-Cheng Hsu, and Wen-Feng Hsieh

Citation: *Applied Physics Letters* **88**, 263117 (2006); doi: 10.1063/1.2218775

View online: <http://dx.doi.org/10.1063/1.2218775>

View Table of Contents: <http://scitation.aip.org/content/aip/journal/apl/88/26?ver=pdfcov>

Published by the *AIP Publishing*

Articles you may be interested in

[Influence of Mn doping on structural, optical, and magnetic properties of Zn_{1-x}Mn_xO nanorods](#)

J. Appl. Phys. **108**, 044910 (2010); 10.1063/1.3478709

[Raman-active Fröhlich optical phonon mode in arsenic implanted ZnO](#)

Appl. Phys. Lett. **94**, 011913 (2009); 10.1063/1.3067997

[Self-assembled ZnO quantum dots with tunable optical properties](#)

Appl. Phys. Lett. **89**, 023122 (2006); 10.1063/1.2221892

[Size dependence of photoluminescence and resonant Raman scattering from ZnO quantum dots](#)

Appl. Phys. Lett. **88**, 261909 (2006); 10.1063/1.2217925

[Origin of the optical phonon frequency shifts in ZnO quantum dots](#)

Appl. Phys. Lett. **86**, 053103 (2005); 10.1063/1.1861509

The advertisement features a dark blue background with white and orange text. At the top left, it reads 'NEW! Asylum Research MFP-3D Infinity™ AFM' in large white letters, followed by 'Unmatched Performance, Versatility and Support' in orange. On the right, the Oxford Instruments logo is shown with the tagline 'The Business of Science®'. Below the text are several images: a textured surface, a circular pattern, a grid of small squares, and the physical AFM instrument. Text boxes describe the instrument's performance, ease of use, and range of accessories.

NEW! Asylum Research MFP-3D Infinity™ AFM
Unmatched Performance, Versatility and Support

OXFORD INSTRUMENTS
The Business of Science®

Stunning high performance

Simpler than ever to GetStarted™

Comprehensive tools for nanomechanics

Widest range of accessories for materials science and bioscience

Band gap engineering and spatial confinement of optical phonon in ZnO quantum dots

Kuo-Feng Lin, Hsin-Ming Cheng,^{a)} Hsu-Cheng Hsu, and Wen-Feng Hsieh^{b)}

Department of Photonics, Institute of Electro-Optical Engineering, National Chiao Tung University, 1001 Tahsueh Road, Hsinchu, Taiwan 30050, Republic of China

(Received 9 March 2006; accepted 27 May 2006; published online 30 June 2006)

Both band gap engineering and spatial confinement of optical phonon were observed depending upon the size of ZnO quantum dots at room temperature. Size-dependent blueshifts of photoluminescence and absorption spectra reveal the quantum confinement effect. The measured Raman spectral shift and asymmetry for the $E_2(\text{high})$ mode caused by localization of optical phonons agree well with that calculated by using the modified spatial correlation model. © 2006 American Institute of Physics. [DOI: 10.1063/1.2218775]

Recent remarkable crystal growth techniques for the fabrication of nanostructured optical devices operating in the ultraviolet (UV), using zinc oxide (ZnO) as the constituent material,^{1–4} have prompted studies into the properties of this promising material in its powder and nanocrystalline forms. In nanocrystals, the quantum confinement effect becomes a predominant investigation field and gives rise to many interesting electronic and optical properties.^{5–11} The phenomena concerning the quantum confinement effect in ZnO nanocrystals were rarely studied due to the relatively large electron effective mass caused by the large band gap (3.37 eV) of this material. Additionally, the Coulomb interaction of electron and hole has reduced the exciton confinement energy partly due to the small dielectric constant $\epsilon_{\infty}^{\text{bulk}}$ in this system, which is also related to large band gap. Thus, the ZnO binary semiconductor material will have a small quantum confinement effect in quantum dot (QD) and quantum well (QW) structures.

ZnO has a wurtzite crystal structure that belongs to the space group C_{6v}^4 and group theory predicts zone-center optical phonon modes, which are A_1 , $2B_1$, E_1 , and $2E_2$. The A_1 and E_1 modes and the two E_2 modes are Raman active while the B modes are silent. The nonpolar E_2 phonon modes have two frequencies: $E_2(\text{high})$ is associated with the vibration of oxygen atoms and $E_2(\text{low})$ is associated with the Zn sublattice. All described phonon modes have been reported in the Raman spectra^{12,13} of bulk ZnO. The Raman spectra always show a shift of phonon frequencies in ZnO nanostructures.^{14–17} Whether the origin of this shift is due to strain, intrinsic defects or the size of QDs is still the subject of debates. Nevertheless, by examining ZnO nanocrystals with average sizes of 8.5 and 4.0 nm, Rajalakshmi *et al.*¹⁷ explained the shift of phonon frequency as due to optical phonon confinement in ZnO nanostructures, without considering the effects of crystallite size distribution (CSD) on the Raman spectra in ZnO nanostructures.

In this letter, we present a quantum confinement effect revealing a blueshift in absorption and PL spectra with a small defect emission for ZnO QDs having the average size

varying from 12 to 3.5 nm in diameter. Furthermore, we observed spatial confinement of the optical phonon induced spectral shift, broadening, and asymmetry of the $E_2(\text{high})$ phonon mode by using typical Raman spectroscopy. We also used the modified spatial correlation (SC) model, which takes the CSD into consideration, that gave a good fit to the measured Raman spectra.

The synthesis of ZnO QDs was carried out using the sol-gel method, which is similar to those published elsewhere.^{18,19} Stoichiometric zinc acetate dihydrate [99.5% Zn(OAc)₂·2H₂O, Riedel-deHaen] was first dissolved into diethylene glycol [99.5% DEG, ethylenediamine-tetra-acetic acid (EDTA)]. The resultant solution was put in a centrifuge operating at 3000 rpm for 30 min and a transparent solution was then obtained containing dispersed single crystalline ZnO QDs. Finally, the supernatant was dropped on a Si(001) substrate with native oxide and dried at 150 °C. The average size of ZnO QDs ranging from 3.5 to 12 nm can be tailored under a well-controlled concentration (0.04–0.32M) of the precursor. The average crystallite size was determined as in the previous report¹⁸ using a Bede D1 x-ray diffractometer with grazing incidence and a JEOL JEM-2100F field emission transmission electron microscope (FETEM) operated at 200 keV. Micro-Raman spectroscopy was carried out by a frequency-doubled Yb:YAG (yttrium aluminium garnet) laser ($\lambda=515$ nm) as a pump source and detected by a Jobin-Yvon T64000 microspectrometer with a 1800 grooves/mm grating in the backscattering configuration.

Figure 1 shows typical photoluminescence (PL) and absorption spectra of the samples with different average QD sizes at room temperature. The UV emission represents a relaxed state of the exciton near the band edge in the ZnO QDs. The nature of the UV-PL from ZnO QDs itself is still a matter of controversy. Some authors attributed the UV-PL to the recombination of confined excitons,²⁰ while others argued that the emission comes from surface impurities or defects.²¹ In our case, high efficient UV emission near the band edge is attributed to confined exciton emission, similar to that described in Ref. 20, with high density of states that shifts to the higher energies from 3.30 to 3.43 eV as the size of QDs decreases from 12 to 3.5 nm, which are comparable or smaller than the diameter (4.68 nm) of the exciton (Bohr radius of bulk ZnO is 2.34 nm).⁶ Additionally, the slight widening in the full width at half maximum (FWHM) of UV

^{a)} Also at: Material and Chemical Research Laboratories, Industrial Technology Research Institute, Hsinchu, Taiwan 310, Republic of China.

^{b)} Author to whom correspondence should be addressed; electronic mail: wfhshieh@mail.nctu.edu.tw

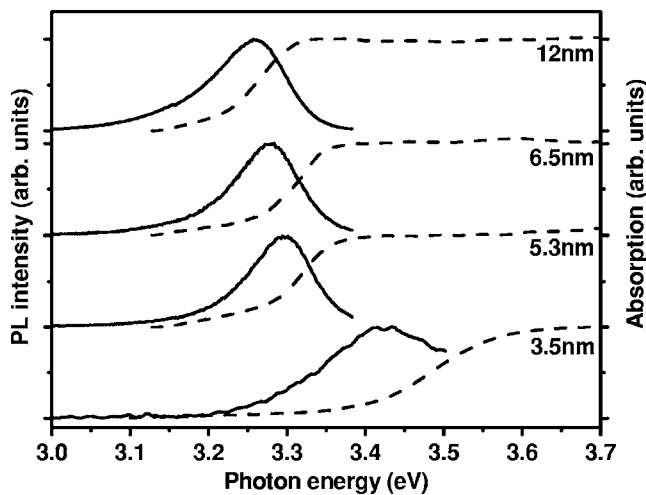


FIG. 1. PL (solid line) and absorption (dashed line) spectra near the band edge of various ZnO QD sizes.

emission with decrease in the size of ZnO QDs may be caused by the recombination of surface-bound acceptor exciton complexes as evident from the lower energy shoulder.²² In general, quantum confinement will widen the energy band gap and give rise to a blueshift in the transition energy as the crystal size decreases. Such a phenomenon is also revealed in the absorption spectra, although the faint excitonic absorption peaks are due to the moderate size distribution of ZnO QDs. From this figure it can clearly be seen that the absorption onset exhibits a progressive blueshift from 3.43 to 3.65 eV as the size of ZnO QD decreases from 12 to 3.5 nm. We calculated the band gaps by using the effective-mass model¹⁸ for different sizes of ZnO QDs and the results showed good agreement with the experimental data.

In order to observe the optical phonon confinement effect, the measured micro-Raman spectra with different sizes of ZnO QDs are shown in Fig. 2 under a fixed excitation laser power of 3.1 mW. We can see that the Raman peak at 300 cm^{-1} , which comes from the Si substrate,²³ stays unshifted in frequency. On the other hand, we found the spectral peak of $E_2(\text{high})$ optical phonon around 435 cm^{-1} to shift to the lower frequency as the size of ZnO QDs decreases. Compared with that of the ZnO bulk, a redshift

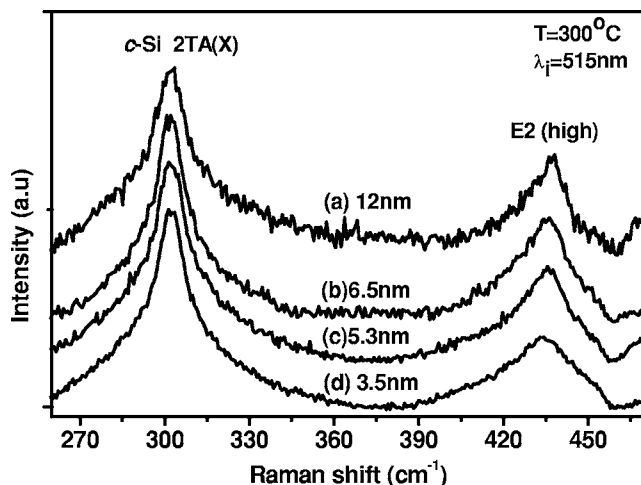


FIG. 2. Typical Raman spectra of different sizes of ZnO QDs: (a) 12 nm, (b) 6.5 nm, (c) 5.3 nm, and (d) 3.5 nm.

ranging from 0.8 to 4.7 cm^{-1} and an asymmetry (Γ_a/Γ_b) from 1.36 to 1.95 were obtained as the QD size decreases from 12 to 3.5 nm. Note that Γ_a and Γ_b are, respectively, the half widths on the low- and high-energy sides of the $E_2(\text{high})$ mode. Such a pronouncing shift, broadening, and the asymmetry of the $E_2(\text{high})$ peak could result from three main mechanisms:¹⁵ (1) phonon localization by intrinsic defects, (2) laser heating in nanostructure ensembles, and (3) the spatial confinement within the dot boundaries. The frequency shift of the phonon resulting from defects should not depend upon the size of quantum dots as also indicated by the small defect PL emission observed in our samples; therefore, we may exclude the defect phonon localization. Additionally, no shift to the $E_2(\text{high})$ peak was observed in all ZnO QDs as the laser power has been varied almost an order of magnitude from 1.5 to 12 mW with a fixed laser spot size of about $2\text{ }\mu\text{m}^2$. It is therefore concluded that the Raman shift is mainly due to the spatial confinement of the optical phonon.

The phonon eigenstates are plane waves with infinite correlation lengths in an ideal crystal, therefore, the Raman scattering can only be observed with phonons around the Brillouin zone center ($q=0$) due to the momentum conservation law. As the crystallite is reduced to nanoscale sizes, the momentum conservation law associated with the Raman scattering can be relaxed and that leads to the spectral shift, broadening, and asymmetry of the Raman modes. The Raman shift and broadening of ZnMnO nanoparticles²⁴ had been evaluated based on the SC model.²⁵ Because the phonon wave function is partially confined to the volume of the crystallite and if a spherical shape of finite size ZnO QDs is assumed, the first-order Raman spectrum $I(\omega)$ can be described by the following equation:²⁵

$$I(\omega) \propto \int_0^1 \frac{4\pi q^2 \exp(-q^2 L^2/4) dq}{[\omega - \omega(q)]^2 + (\Gamma/2)^2}, \quad (1)$$

where q is expressed in units of $2\pi/a$, a is the lattice constant, $\omega(q)$ is the phonon dispersion relation, Γ is the linewidth of $E_2(\text{high})$ phonon of the bulk ZnO, and L is spatial correlation length corresponding to grain size. Furthermore, Islam *et al.*^{26,27} reported that CSD influenced both the shifts in Raman scattering frequencies and line shapes in silicon nanostructures. They modified the Raman intensity expression, $I(\omega)$ of Eq. (1), to $I(\omega, L_0, \sigma)$ by using a Gaussian CSD of an ensemble of spherical crystallites with mean crystallite size L_0 and standard deviation σ . After integrating the results over the crystallite sizes L under the condition $L_0 > 3\sigma$, the total Raman intensity expression for the whole ensemble of nanocrystallites becomes

$$I(\omega) \propto \int_0^1 \frac{f(q) q^2 \exp(-q^2 L_0^2/4) dq}{[\omega - \omega(q)]^2 + (\Gamma/2)^2}, \quad (2)$$

where $f(q) = 1/\sqrt{1+q^2\sigma^2/2}$ is the characteristics of the CSD. The calculated normalization Raman profiles from an ensemble of ZnO QDs having a mean crystallite size $L_0 = 6.5\text{ nm}$ with varying σ to illustrate the effect of σ on the Raman line shape are plotted in Fig. 3. It is clear that a single crystalline component with $\sigma=0.27$ describes the Raman spectra of 6.5 nm ZnO QDs quite well. Additionally, the CSD of all samples were about 27%, which agrees with the TEM result,¹⁸ e.g., the obtained crystal size of $4.3 \pm 1.1\text{ nm}$. The frequency shift $\Delta\omega$ and the asymmetry, Γ_a/Γ_b , of

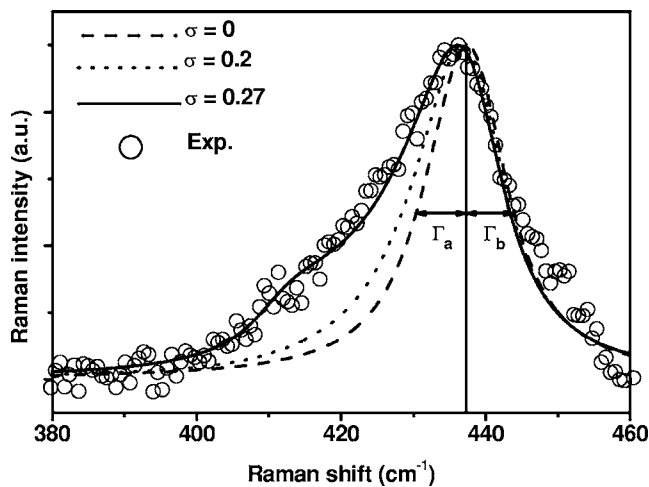


FIG. 3. Fitting of the modified spatial correlation model with $\sigma=0$, 0.2, and 0.27, respectively, to the measured result for average size of 6.5 nm ZnO QDs.

$E_2(\text{high})$ mode from the ZnO bulk (439 cm^{-1}) as a function of diameter or correlation length with $\sigma=0.27$ were plotted in Fig. 4, in which the solid curves indicate the calculated results of the modified SC model and the hollow circles the experimental results. We found that the measured frequency shift and asymmetry agrees very well with the ones calculated by the modified SC model and the mean values of crystallite sizes obtained from our fitting are also in good agreement with the XRD results.

In summary, size dependence of efficient UV photoluminescence and absorption spectra of various ZnO QD sizes give evidence for the quantum confinement effect. We have observed the spectral shift, broadening, and asymmetry of the optical phonons for different sizes of ZnO QDs and clarified that the origin of these effects is spatial confinement of phonon in ZnO QDs. Using the modified spatial correlation

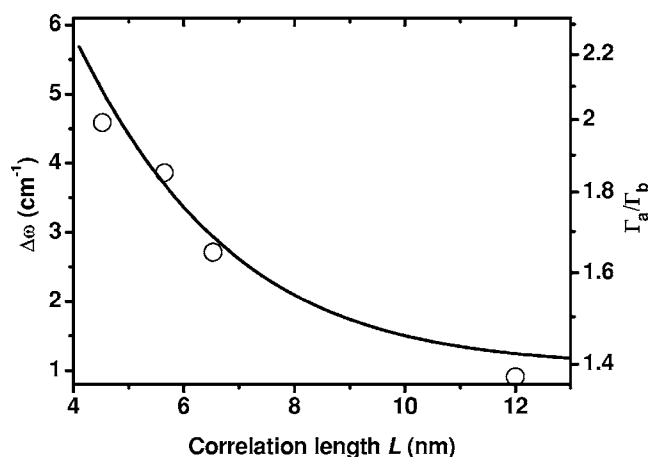


FIG. 4. Raman shift $\Delta\omega$ and asymmetric broadening Γ_a/Γ_b of $E_2(\text{high})$ phonon as a function of correlation length L or average size of nanocrystal. The solid curves indicate the calculated results of the modified SC model and the hollow circles the experimental results.

model to analyze the broadening and asymmetry of the first-order $E_2(\text{high})$ phonon mode, we further confirmed the phonon confinement based on the finite correlation length of a propagating phonon.

The authors would like to gratefully acknowledge partial financial support from the National Science Council (NSC) of Taiwan under Contract No. NSC-94-2112-M-009-021. One of the authors (H.C.H.) acknowledges NSC of Taiwan for providing a fellowship. The authors also thank Lai of the TEM group of Material Research Laboratory in ITRI for the help on electron microscopy measurements.

- ¹L. B. Kong, F. Li, L. Y. Zhang, and X. Yao, *J. Mater. Sci. Lett.* **17**, 769 (1998).
- ²R. L. Hoffman, B. J. Norris, and J. F. Wager, *Appl. Phys. Lett.* **82**, 733 (2003).
- ³R. Könenkamp, R. C. Word, and C. Schlegel, *Appl. Phys. Lett.* **85**, 6004 (2004).
- ⁴J. B. Baxter and E. S. Aydil, *Appl. Phys. Lett.* **86**, 053114 (2005).
- ⁵T. Kawazoe, K. Kobayashi, and M. Ohtsu, *Appl. Phys. Lett.* **86**, 103102 (2005).
- ⁶R. T. Senger and K. K. Bajaj, *Phys. Rev. B* **68**, 045313 (2003).
- ⁷T. A. Klar, T. Franzl, A. L. Rogach, and J. Feldmann, *Adv. Mater. (Weinheim, Ger.)* **17**, 769 (2005).
- ⁸Y. Gu, Igor L. Kuskovsky, M. Yin, S. O'Brien, and G. F. Neumark, *Appl. Phys. Lett.* **85**, 3833 (2004).
- ⁹R. P. Wang, G. Xu, and P. Jin, *Phys. Rev. B* **69**, 113303 (2004).
- ¹⁰V. V. Ursaki, I. M. Tiginyanu, V. V. Zalamai, E. V. Rusu, G. A. Emelchenko, V. M. Masalov, and E. N. Samarov, *Phys. Rev. B* **70**, 155204 (2004).
- ¹¹H. M. Cheng, K. F. Lin, H. C. Hsu, C. J. Lin, L. J. Lin, and W. F. Hsieh, *J. Phys. Chem. B* **109**, 18385 (2005).
- ¹²J. F. Scott, *Phys. Rev. B* **2**, 1209 (1970).
- ¹³N. Ashkenov, B. N. Mbenkum, C. Bundesmann, V. Riede, M. Lorenz, D. Spemann, E. M. Kaidashev, A. Kasic, M. Schubert, M. Grundmann, G. Wagner, H. Neumann, V. Darakchieva, H. Arwin, and B. Monemar, *J. Appl. Phys.* **93**, 126 (2003).
- ¹⁴L. Bergman, X. B. Chen, J. L. Morrison, and J. Huso, *J. Appl. Phys.* **96**, 675 (2004).
- ¹⁵K. A. Alim, V. A. Fonoberov, and A. A. Balandin, *Appl. Phys. Lett.* **86**, 053013 (2005).
- ¹⁶K. A. Alim, V. A. Fonoberov, M. Shamsa, and A. A. Balandin, *J. Appl. Phys.* **97**, 124313 (2005).
- ¹⁷M. Rajalakshmi, A. K. Arora, B. S. Bendre, and S. Mahamuni, *J. Appl. Phys.* **87**, 2445 (2000).
- ¹⁸K. F. Lin, H. M. Cheng, H. C. Hsu, L. J. Lin, and W. F. Hsieh, *Chem. Phys. Lett.* **409**, 208 (2005).
- ¹⁹H. M. Cheng, H. C. Hsu, S. L. Chen, W. T. Wu, C. C. Kao, L. J. Lin, and W. F. Hsieh, *J. Cryst. Growth* **277**, 192 (2005).
- ²⁰D. W. Bahnemann, C. Kormann, and M. R. Hoffmann, *J. Phys. Chem.* **91**, 3789 (1987).
- ²¹L. Guo, S. Yang, C. Yang, P. Yu, J. Wang, W. Ge, and G. K. L. Wong, *Appl. Phys. Lett.* **76**, 2901 (2000).
- ²²V. A. Fonoberov and A. A. Balandin, *Appl. Phys. Lett.* **85**, 5971 (2004).
- ²³R. P. Wang, G. W. Zhou, Y. L. Liu, S. H. Pan, H. Z. Zhang, and D. P. Yu, *Phys. Rev. B* **61**, 16 827 (2000).
- ²⁴J. B. Wang, H. M. Zhong, Z. F. Li, and Wei Lu, *J. Appl. Phys.* **97**, 086105 (2005).
- ²⁵H. Richter, Z. P. Wang, and L. Ley, *Solid State Commun.* **39**, 625 (1981); I. H. Campbell and P. M. Fauchet, *ibid.* **58**, 739 (1986).
- ²⁶Md. N. Islam and S. Kumar, *Appl. Phys. Lett.* **78**, 715 (2001).
- ²⁷Md. N. Islam, A. Pradhan, and S. Kumar, *J. Appl. Phys.* **98**, 024309 (2005).